

The K20 Survey: New Light on Galaxy Formation and Evolution

A. CIMATTI¹, E. DADDI², M. MIGNOLI³, L. POZZETTI³, A. FONTANA⁴, T. BROADHURST⁵, F. POLI⁶, P. SARACCO⁷, A. RENZINI², G. ZAMORANI³, N. MENCI⁴, S. CRISTIANI⁸, S. D'ODORICO², E. GIALLONGO⁴, R. GILMOZZI², S. DI SEREGO ALIGHIERI¹, J. VERNET¹

¹INAF – Osservatorio Astrofisico di Arcetri, Italy; ²European Southern Observatory, Garching, Germany;

³INAF – Osservatorio Astronomico di Bologna, Italy; ⁴INAF – Osservatorio Astronomico di Roma, Italy;

⁵Racah Institute for Physics, The Hebrew University, Jerusalem, Israel; ⁶Dipartimento di Astronomia, Università

di Roma, Italy; ⁷INAF – Osservatorio Astronomico di Brera, Italy; ⁸INAF – Osservatorio Astronomico di Trieste, Italy

1. Introduction

Despite the recent extraordinary progress in observational cosmology and the successful convergence on a single cosmological model, the history of galaxy and structure formation and evolution remains still an open question. One of the most actively debated issues is how and when the present-day most massive galaxies (e.g. elliptical galaxies and bulges with $\mathcal{M}_{\text{stars}} > 10^{11} M_{\odot}$) built up and what type of evolution characterized their growth over the cosmic time. Addressing this question is important not only to test the different scenarios of galaxy formation, but also to understand how the general structures of the universe evolved.

There is wide consensus that galaxy formation takes place by a combination of dissipational collapse and merging of sub-units (e.g. White & Rees 1978). However, much less consensus presently exists on the main epoch (redshift) at which these events took place, and then when the bulk of the stellar mass of present-day galaxies was formed and assembled. Hierarchical merging models (HMMs) have so far favoured a rather late appearance of massive galaxies, thus only quite recently reaching their present mass, i.e., at $z < 1-1.5$ (e.g. Baugh et al. 2002). On the other hand, other scenarios and some observational evidence suggest that the bulk of star formation and galaxy assembly took place at substantial higher redshifts (see Cimatti 2003 for a recent review). Such scenarios make very different predictions depending on the formation epoch. If massive galaxies formed at $z > 2-3$ through a short-lived and intense starburst phenomenon followed by a passive and pure luminosity evolution (PLE), then old (a few Gyr) passively evolving massive systems should exist up to $z \sim 1-1.5$ with a number density identical to that observed in the local universe because their number does not change through cosmic time and the only evolution is the aging of the stellar population. On the other hand, if the most massive galaxies reach their final mass at $z < 1-1.5$, they should be

rare at $z \sim 1-1.5$, with a comoving density of $\mathcal{M}_{\text{stars}} > 10^{11} M_{\odot}$ galaxies decreasing by almost an order of magnitude from $z \sim 0$ to $z \sim 1$ (Baugh et al. 2002).

Although there is a general agreement on *cluster* ellipticals being a homogeneous population of old and passive systems formed at high redshifts (see Renzini 1999 and Peebles 2002 for recent reviews), the question of *field* spheroids is still controversial. Several observations were performed over recent years in order to test the two competing models. However, although it is established that old, passive and massive systems exist in the field out to $z \sim 1.5$, there is not yet agreement on how their number and evolutionary properties compare with the model predictions.

2. The K20 Survey

A solid and unbiased approach to investigate the evolution of massive

galaxies is to study samples of field galaxies selected in the K-band (i.e. at $2.2 \mu\text{m}$; Broadhurst et al. 1992; Kauffmann & Charlot 1998). This has two main advantages. Firstly, since the rest-frame optical and near-IR light is a good tracer of the galaxy *stellar* mass (Gavazzi et al. 1996), K-band surveys select galaxies according to their mass up to $z \sim 2$. Secondly, the similarity of the spectral shapes of different galaxy types in the rest-frame optical/near-IR makes the K-band selection free from strong biases against or in favour of particular classes of galaxies. In contrast, the selection of high- z galaxies in the observed optical bands is sensitive to the star-formation activity rather than to the stellar mass because it samples the rest-frame UV light and makes optical samples biased against old passive galaxies.

Motivated by the above open questions and by the availability of the ESO VLT telescopes, we started an ESO VLT Large Programme (dubbed “K20

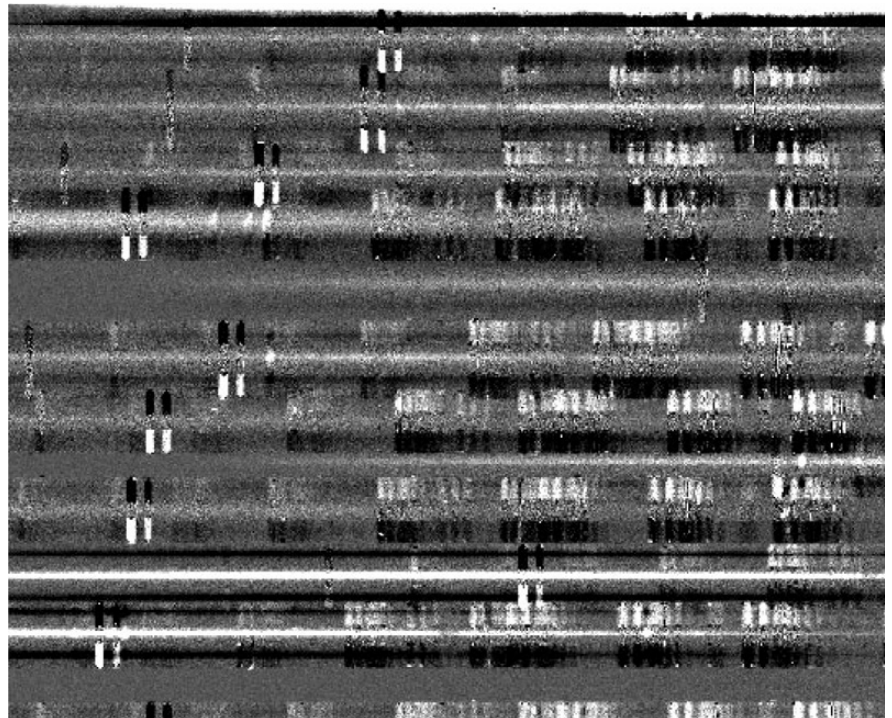


Figure 1: Zoom on two-dimensional sky-subtracted spectra of faint galaxies present in a section of one of the FORS2 MXU masks used for the “dithered” observations.

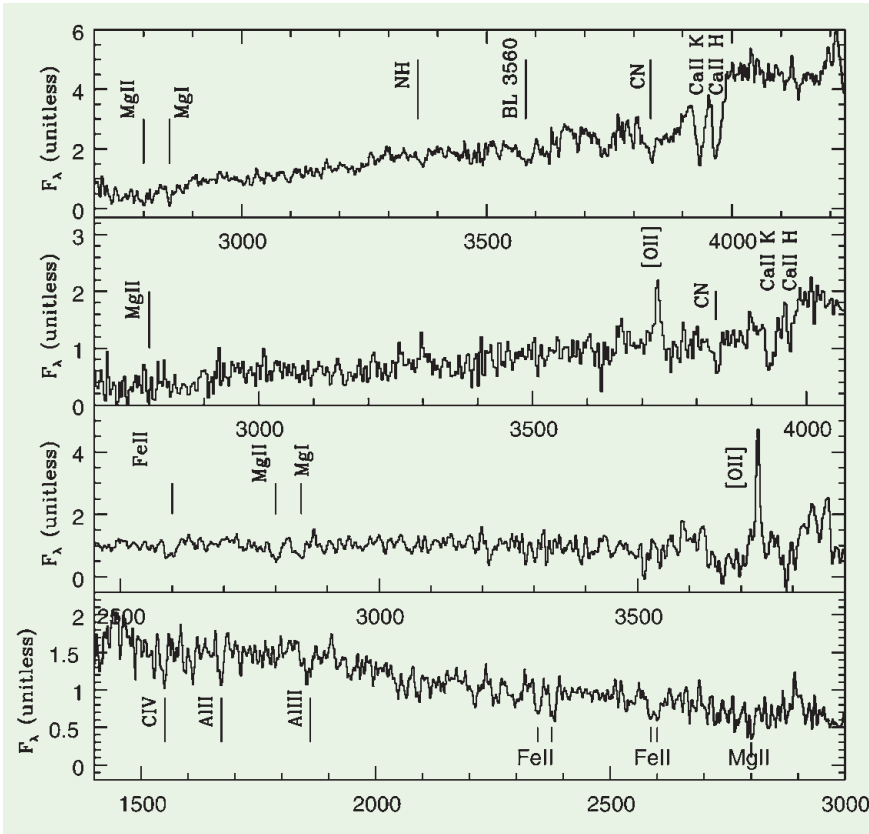


Figure 2: Examples of FORS2 spectra of high- z galaxies with the four adopted spectral classifications. From top to bottom: an early-type at $z = 1.096$ ($R = 23.0$), an early-type + $[\text{OII}]\lambda 3727$ emission at $z = 0.735$ ($R = 23$), an emission line galaxy at $z = 1.367$ ($R = 23.0$), an absorption line galaxy at $z = 1.725$ ($R = 23.5$).

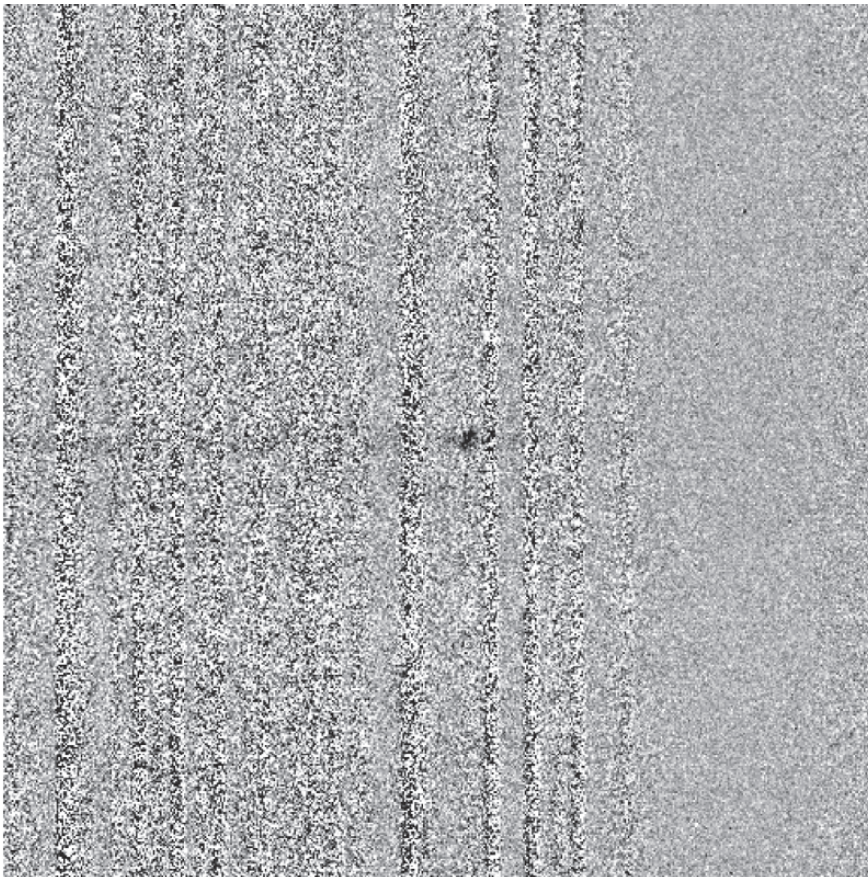


Figure 3: ISAAC two-dimensional sky-subtracted H-band low-resolution spectrum of a galaxy at $z = 1.73$ (the emission line is $H\alpha$).

survey”) based on 17 nights distributed over two years (1999–2000) (see <http://www.arcetri.astro.it/~k20/> and Cimatti et al. 2002c). The prime aim of this survey was to derive the spectroscopic redshift distribution and the spectral properties of 546 K_s -selected objects with the *only* selection criterion being $K_s < 20$ (Vega scale). Such a threshold is critical because it selects galaxies over a broad range of masses, i.e. $\mathcal{M}_{\text{stars}} > 10^{10} M_{\odot}$ and $\mathcal{M}_{\text{stars}} > 4 \times 10^{10} M_{\odot}$ for $z = 0.5$ and $z = 1$ respectively. The targets were selected from K_s -band images (ESO NTT+SOFI) of two independent fields covering a total area of 52 arcmin²: a 32.2 arcmin² sub-area of the Chandra Deep Field South (CDFs; Giacconi et al. 2001), and a 19.8 arcmin² field centred around the QSO 0055-269 at $z = 3.6$. Extensive simulations showed that the sample is photometrically highly complete to $K_s = 20.0$ and not affected by strong selection effects on the galaxy populations, with the exception of an underestimate of ~ 0.2 magnitudes for the luminous galaxies (Cimatti et al. 2002c). $H_0 = 70 \text{ km s}^{-1} \text{ Mpc}^{-1}$, $\Omega_m = 0.3$ and $\Omega_{\Lambda} = 0.7$ are adopted throughout this article.

3. The VLT Observations: Optimizing Spectroscopy for Faint Red Galaxies

The most crucial probes of massive galaxy evolution are galaxies with the very red colours expected for passively evolving systems at $z > 1$ (e.g. $R - K_s > 5$). For $K_s < 20$, such red colours imply very faint optical magnitudes ($R \sim 24\text{--}26$), close to the spectroscopic limits of 8-m-class telescopes. Moreover, the most prominent spectral features (e.g. the 4000 Å break and H&K absorptions) fall in the very red part of the observed spectra for $1 < z < 2$ ($\lambda_{\text{obs}} > 8000 \text{ Å}$), where the strong OH sky lines and the CCD fringing (very strong in FORS2 before its recent upgrade of March 2002 with new red-optimized MIT CCD mosaic) make the spectroscopy of faint $z > 1$ galaxies extremely challenging.

For such reasons, the spectroscopy was optimized to reach the highest possible signal-to-noise ratio in the red by applying the innovative technique of “dithering” the targets along the slits every 15–20 minutes between two (or more) fixed positions. Such a method (routinely used in the near-IR) has the crucial advantage of efficiently subtracting both the CCD fringing and the OH sky lines. A similar method can also be performed with the so-called “nod and shuffle” technique by nodding the telescope rapidly between targets and adjacent sky positions and recording object and sky spectra on adjacent regions of a low-noise CCD through charge shuffling. At the time of the observations, no automatic templates

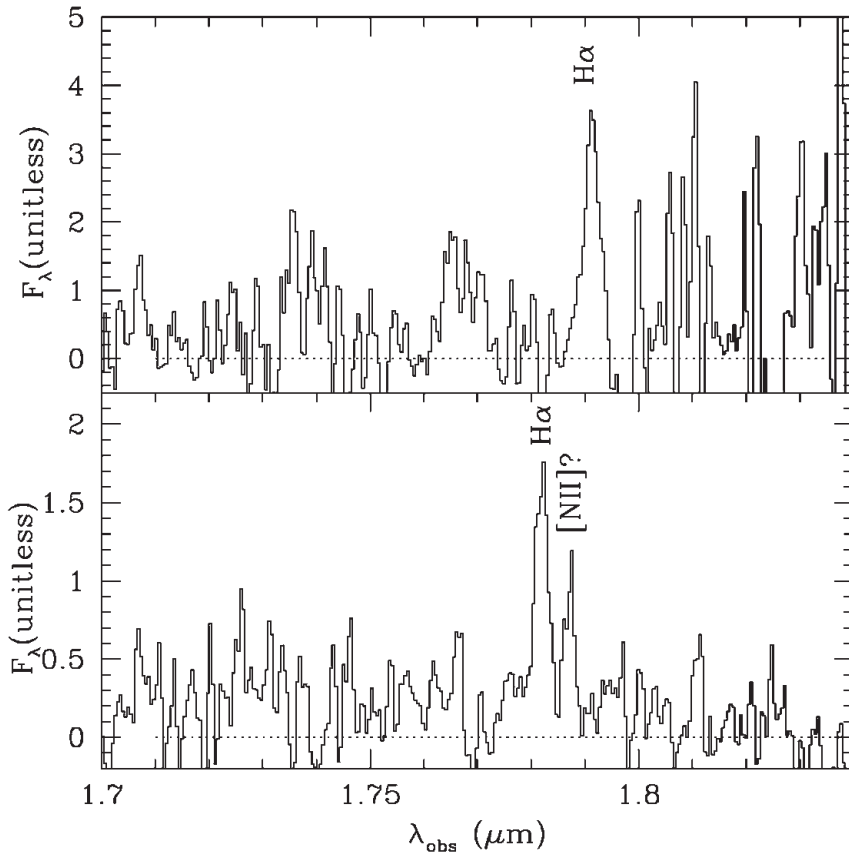


Figure 4: ISAAC H-band low resolution spectra of two emission-line galaxies with $H\alpha$ redshifted at $z = 1.729$ (top panel) and $z = 1.715$ (bottom panel).

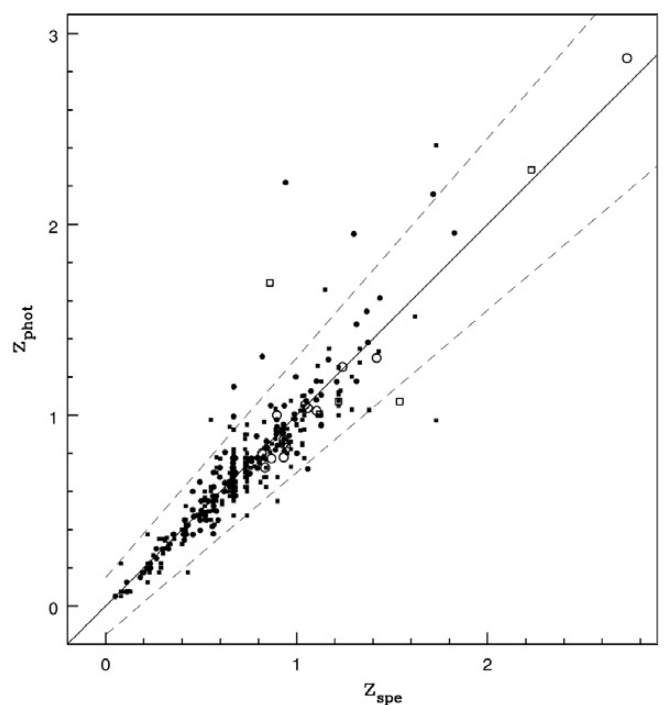
were available to perform dithered observations with FORS2, but we succeeded in applying this technique by moving the telescope “manually” from one position to another thanks to the kind help of the support astronomers. Our approach proved to be very successful in achieving high-quality spectra extended to the far red (Fig. 1) and reaching a spectroscopic redshift completeness for the high- z red galaxies much higher than in previous surveys.

Optical multi-object spectroscopy was obtained with the ESO VLT UT1 and UT2 equipped respectively with FORS1 (with the MOS mode: 19 movable slitlets) and FORS2 (with the Mask Exchange Unit, MXU, mode). The MXU mode uses laser-cut slit masks prepared by the mask manufacturing unit (MMU), and allowed us to observe up to 52 targets per mask with slit lengths of 8”–15” (a “record” for the multiplex in the pre-VIMOS era!). The seeing and the slit widths were in the range of 0.5”–2.0” and 0.7”–1.2” respectively. The integration times ranged from 0.5 to 3 hours. Figure 2 shows some typical spectra.

A fraction of the sample was also observed with near-IR spectroscopy using VLT UT1 + ISAAC in low-resolution mode with a 1” slit, 1–3 hours integration times, 1–2 targets per slit, in order to attempt to derive the redshifts of the galaxies which were too faint for optical

spectroscopy and/or expected to be in a redshift range without strong features in the observed spectral range (e.g. $1.4 < z < 2.0$). However, the absence of a multiobject spectroscopic mode, each integration being limited to a single spectral band, and the lack of very accurate photometric redshifts at the time of the observations made it difficult to derive a substantial number of spectroscopic redshifts based on near-IR spectroscopy alone. Overall, redshifts were de-

Figure 5: The comparison between spectroscopic (x -axis) and photometric (y -axis) redshifts of the galaxies in the K20 survey. Filled circles, filled squares and open symbols indicate the 0055-269 field, the CDFS and the “lower quality” spectroscopic redshifts respectively.



rived for four galaxies at $1.3 < z < 1.9$ out of the 22 observed (Figs. 3–4).

In addition to spectroscopy, $UBVR I z J K_s$ imaging from NTT and VLT observations was also available for both fields, thus providing the possibility to estimate photometric redshifts for all the objects in the K20 sample, to optimize them through a comparison with the spectroscopic redshifts and to assign reliable photometric redshifts to the objects for which it was not possible to derive the spectroscopic redshift. The dispersion on the global sample (CDFS + 0055-269 fields) is $\sigma = 0.089$ and the average is $\langle z_{\text{spe}} - z_{\text{phot}} \rangle = 0.012$ (Fig. 5). Such an accuracy is at the level of the “state-of-the-art” photometric redshifts obtained in the *Hubble Deep Fields*. The final sample covers a redshift range of $0 < z < 2.5$ and the overall spectroscopic redshift completeness is 94%, 92%, 87% for $K_s < 19.0, 19.5, 20.0$ respectively. The overall redshift completeness (spectroscopic and photometric) is 98%.

The K20 survey represents a significant improvement with respect to previous surveys for faint K -selected galaxies (e.g. Cowie et al. 1996; Cohen et al. 1999), thanks to its high spectroscopic redshift completeness, the larger sample, the coverage of two fields (thus reducing the cosmic variance effects), and the availability of optimized photometric redshifts.

4. The Redshift Distribution: Testing Galaxy-Formation Models

The observed differential and cumulative redshift distributions for the K20 sample are presented in Fig. 6 (see Cimatti et al. 2002b), together with the

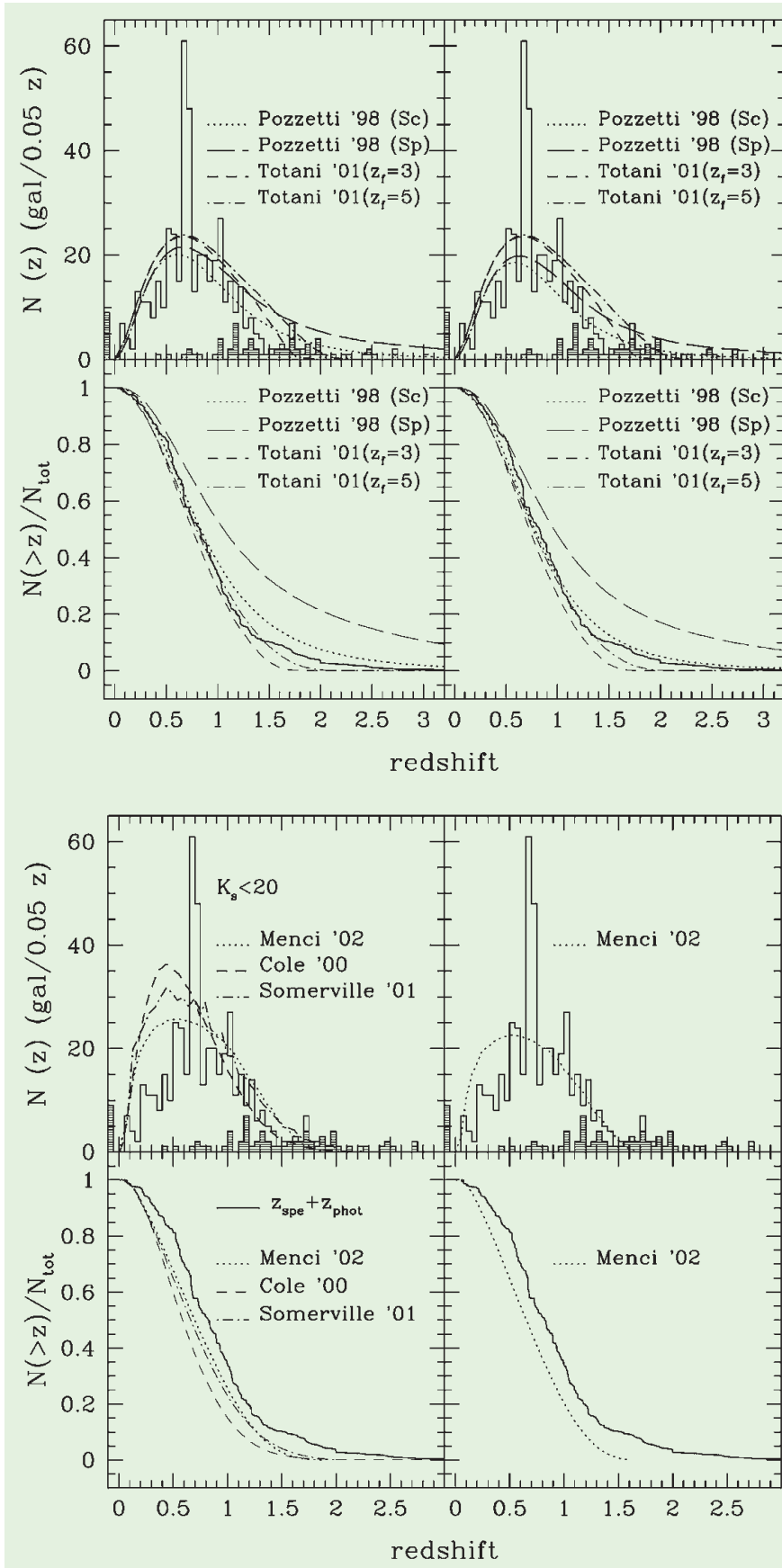


Figure 6a: Top panels: the observed differential $N(z)$ for $K_s < 20$ (histogram) compared with the PLE model predictions. Bottom panels: the observed fractional cumulative redshift distribution (continuous line) compared with the same models. The shaded histogram shows the contribution of photometric redshifts. The bin at $z < 0$ indicates the 9 objects without redshift. The left and right panels show the models without and with the inclusion of the photometric selection effects respectively. Sc and Sp indicate Scalo and Salpeter IMFs respectively. Figure 6b: Same as Fig. 6a, but compared with the HMM predictions. Right panels: the M02 model with the inclusion of the photometric selection effects.

predictions of different scenarios of galaxy formation and evolution, including hierarchical merging models (HMMs) from Menci et al. (2002, M02), Cole et al. (2000, C00), Somerville et al. (2001, S01), and pure luminosity evolution models (PLE) based on Pozzetti et al. (1996, PPLE) and Totani et al. (2001, TPLE). No best tuning of the models was attempted in this comparison, thus allowing an unbiased *blind* test with the K20 observational data. The predicted $N(z)$ from the models are normalized to the K20 survey sky area.

The observed redshift distribution can be retrieved from <http://www.arcetri.astro.it/k20>. The spike at $z \sim 0.7$ is due to two galaxy clusters (or rich groups) at $z = 0.67$ and $z = 0.73$. The median redshift of $N(z)$ is $z_{med} = 0.737$ and $z_{med} = 0.805$, respectively with and without the two clusters being included. The contribution of objects with only a photometric redshift becomes relevant only for $z > 1.5$.

Figure 6a shows fairly good agreement between the observed $N(z)$ distribution and the PLE models (with the exception of PPLE with Salpeter IMF), although such models slightly overpredict the number of galaxies at $z > 1.2$. However, if the photometric selection effects present in the K20 survey (Cimatti et al. 2002c) are taken into account, the PLE models become much closer to the observed $N(z)$ thanks to the decrease of the predicted high- z tail.

In contrast, all the HMMs underpredict the median redshift, overpredict the total number of galaxies with $K_s < 20$ by factors up to $\sim 50\%$ as well as the number of galaxies at $z < 0.5$, and underpredict the fractions of $z > 1-1.5$ galaxies by factors of 2-4 (Fig. 6b). The inclusion of the photometric selection effects (Cimatti et al. 2002c) exacerbates this discrepancy, as shown in Figure 6b (right panels) for the M02 model (the discrepancy for the C00 and S01 models becomes even larger). The deficit of high- z objects in HMMs is well illustrated by Figure 7, where the PPLE model reproduces the cumulative *number* distribution of galaxies at $1 < z < 3$ within $1-2 \sigma$, whereas the M02 model is discrepant at $\geq 3\sigma$ level (up to $> 5\sigma$ for $1.5 < z < 2.5$). This conclusion does not strongly depend on the objects with only photometric redshifts: the 7 galaxies with spectroscopic redshift $z > 1.6$ are already discrepant with the predictions by HMMs of basically no galaxies with $K_s < 20$ and $z > 1.6$.

5. The Luminosity Function and Luminosity Density Evolution

The evolution of galaxies can be investigated through the variation of their number density and luminosity (i.e. the

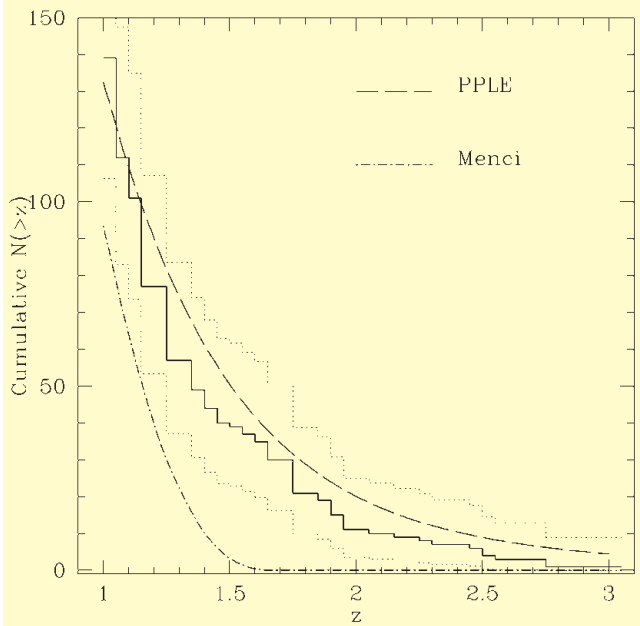
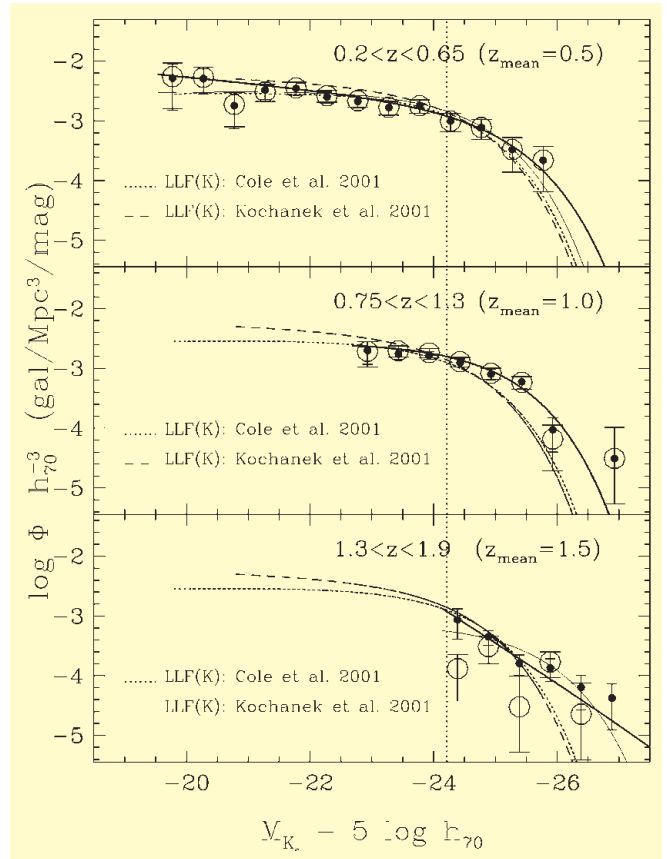


Figure 7: The observed cumulative number of galaxies between $1 < z < 3$ (continuous line) and the corresponding poissonian $\pm 3\sigma$ confidence region (dotted lines). The PPLE (Scalo IMF) and the M02 models are corrected for the photometric biases.

Figure 8: The rest-frame K_s -band Luminosity Function in three redshift bins. Solid curves: the Schechter fits. Dotted curve: the local K_s -band LF of Cole et al. (2001). Open circles: spectroscopic redshifts, filled circles: spectroscopic + photometric redshifts. ▶



luminosity function, LF) over the cosmic time.

The LF of the K20 galaxies has been estimated in the rest-frame K_s -band and in three redshift bins ($z_{\text{mean}} = 0.5, 1.0, 1.5$) in order to trace its evolution (Pozzetti et al. 2003). A comparison with the local universe K_s -band LF of Cole et al. (2001) shows a mild luminosity evolution of LF(z) out to $z = 1$, i.e. the LF shifts along the X-axis as a function of z without an appreciable change in the number density (Y-axis). The brightening is approximately -0.5 magnitudes from $z = 0$ to $z = 1$ (Fig. 8).

The size and completeness of the K20 sample allowed us also to study the LF evolution by galaxy spectral or colour types, and showed that red early-type galaxies dominate the bright end of the LF already at $z \sim 1$, and that their number density shows only a small decrease from $z \sim 0$ to $z \sim 1$ (Pozzetti et al. 2003).

The PLE models describe reasonably well the shape and the evolution of the observed luminosity function up to at least $z_{\text{mean}} = 1.0$, with no evidence for a strong decline in the abundance of the most luminous systems (with $L > L^*$) (Fig. 9b). Hierarchical merging models overpredict faint sub- L^* galaxies at $0 < z < 1.3$, and underpredict the density of luminous ($M_{K_s} < -25.5 + 5 \log h_{70}$) galaxies at the bright end of the LF (Fig. 9a). A comparison between the $R - K_s$ colours and luminosity distributions of K20 galaxies with $0.75 < z < 1.3$ (a bin dominated by spectroscopic red-

shifts) to the predictions of the GIF¹ simulations (Kauffmann et al. 1999) highlights a discrepancy between the two distributions: real luminous galaxies with $M_K - 5 \log h_{70} < -24.5$ in the K20 sample have a median colour of $R - K_s \sim 5$, whereas the GIF simulated galaxies have $R - K_s \sim 4$, with a small overlap of two colour distributions (Fig. 10). This is probably due to an underestimate of $\mathcal{M}_{\text{stars}}/L$ and of the number density of massive galaxies at $z \sim 1$ by the HMMs.

An additional way to investigate galaxy evolution is to trace the integrated cosmic emission history of galaxies at different wavelengths through the study of the luminosity density ρ_λ ($\text{W Hz}^{-1} \text{Mpc}^{-3}$). Such an approach is independent of the details of galaxy evolution and depends mainly on the star-formation history of the universe. Attempts to reconstruct the cosmic evolution of ρ_λ were made previously mainly in the UV and optical bands, i.e. focusing on the star-formation history of galaxies. Our survey offered for the first time the possibility to investigate in the near-IR, thus providing new clues on the global evolution of the stellar mass density (Pozzetti et al. 2003). The results show an evolution of $\rho_\lambda(z) = \rho_\lambda(z=0)(1+z)^{0.37}$, much slower than the one derived in the UV-optical, typically $\propto (1+z)^{3-4}$. Such a slow evolution suggests that the stellar mass density should also evolve slowly at least up to $z \sim 1.3$ (see also Dickinson et al. 2003).

¹<http://www.mpa.garching.mpg.de/GIF/>

The estimate of the stellar mass function and its cosmic evolution is under way and will provide additional constraints on the evolution of massive systems (Fontana et al. 2003, in preparation).

6. Extremely Red Objects (EROs)

As discussed in previous sections, Extremely Red Objects (EROs, i.e. galaxies with $R - K > 5$) are very important because they allow us to select old passively evolving galaxies at $z > 1$. Thanks to our deep red-optimized VLT optical spectroscopy, for a fraction of EROs (70% to $K_s < 19.2$) present in the K20 sample it was possible to derive a spectroscopic redshift and a spectral classification (Cimatti et al. 2002a), thus, for the first time, allowing us to verify if the ERO population is indeed dominated by old passive galaxies. The VLT optical spectra show that two classes of galaxies at $z \sim 1$ contribute nearly equally to the ERO population: the expected old stellar systems, but also a substantial fraction of dusty star-forming galaxies (Fig. 11).

The colours and spectral properties of old EROs are consistent with ≥ 3 Gyr old passively evolving stellar populations (assuming solar metallicity and Salpeter IMF), requiring a formation redshift $z_f > 2.4$ (Fig. 12). The number density is $6.3 \pm 1.8 \times 10^{-4} \text{ h}^3 \text{Mpc}^{-3}$ for $K_s < 19.2$, consistent with the expectations of PLE models for passively evolving early-type galaxies with similar

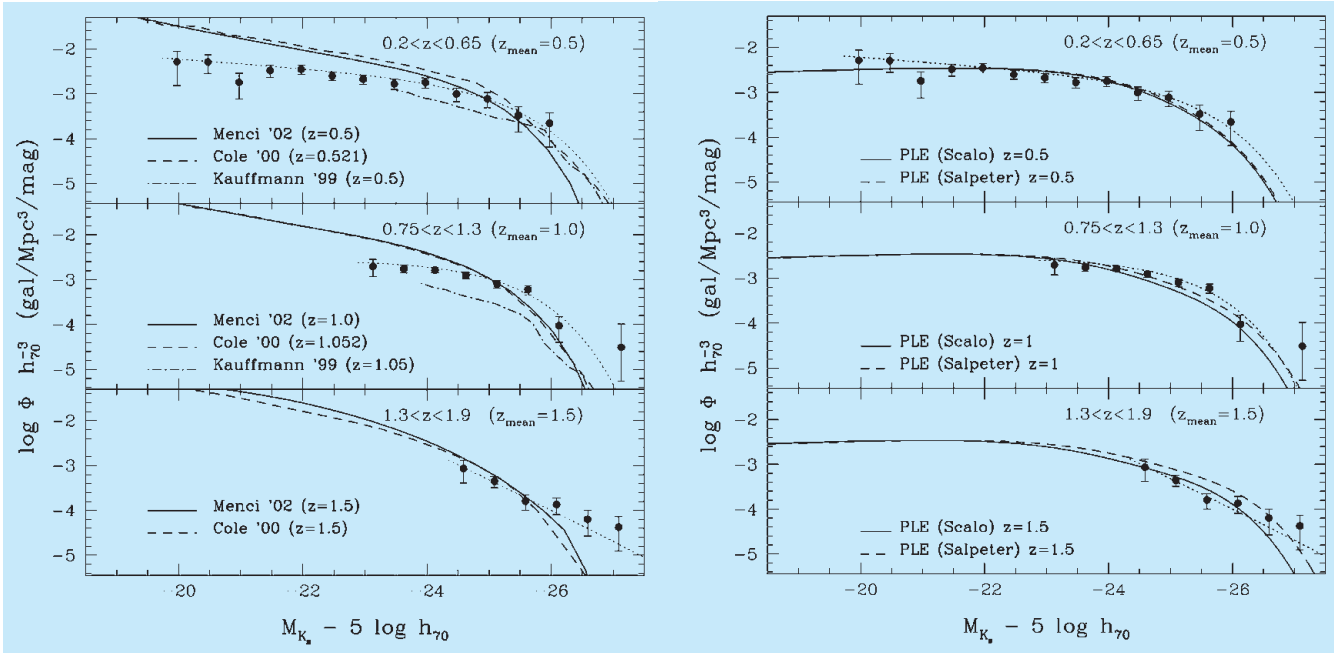


Figure 9a: The K_s -band LF compared to hierarchical merging model predictions. Figure 9b: The K_s -band LF compared to PLE model predictions.

formation redshifts (Cimatti et al. 2002a). HMMs underpredict such old red galaxies at $z \sim 1$ by factors of ~ 3 (Kauffmann et al. 1999) and ~ 5 (Cole et al. 2000).

The spectra of star-forming EROs suggest a dust reddening of $E(B - V) \sim 0.5-1$ (Fig. 12, adopting the Calzetti extinction law), implying typical star-formation rates of $50-150 M_{\odot} \text{yr}^{-1}$, and a significant contribution ($> 20-30\%$) to the cosmic star-formation density at $z \sim 1$. Such dusty star-forming systems are also underpredicted by HMMs. For instance, the GIF simulations predict a comoving density of red galaxies with $SFR > 50 M_{\odot} \text{yr}^{-1}$ that is ~ 30 times lower than the observed density of dusty EROs.

Taking advantage of the spectroscopic redshift information for the two ERO classes, we compared the relative 3D clustering in real space (Daddi et al. 2002). The comoving correlation lengths of dusty and old EROs are constrained to be $r_0 < 2.5$ and $5.5 < r_0 < 16 h^{-1} \text{Mpc}$ comoving respectively, implying that old EROs are the main source of the ERO strong angular clustering. It is important to notice that the strong clustering measured for the old EROs is in agreement with the predictions of hierarchical merging (Kauffmann et al. 1999).

7. Summary and Outlook

The high level of redshift completeness of the K20 survey and the results presented in previous sections provide new implications for a better understanding of the evolution of “mass-selected” field galaxies.

Overall, the results of the K20 survey show that galaxies selected in the

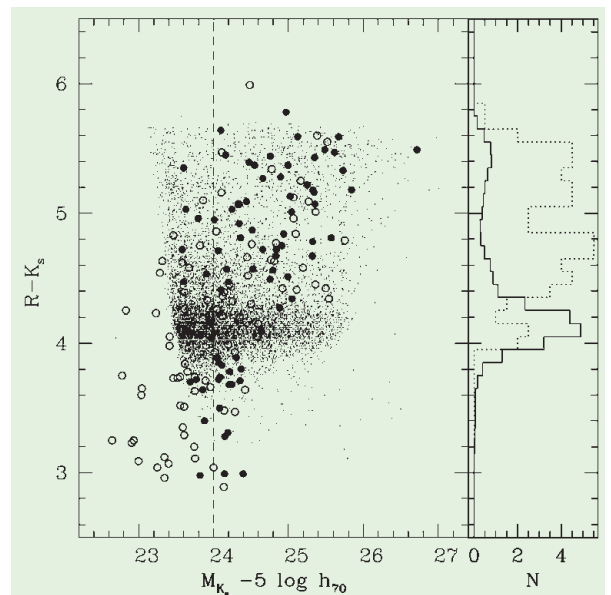
K_s -band are characterized by little evolution up to $z \sim 1$, and that the observed properties can be successfully described by a PLE scenario. In contrast, HMMs fail in reproducing the observations because they predict a sort of “delayed” scenario in which the assembly of massive galaxies occurs later than actually observed. However, it is important to stress here that the above results do not necessarily mean that the whole framework of hierarchical merging of CDM halos is under discussion. For instance, the strong clustering of old EROs and the clustering evolution of the K20 galaxies (irrespective of colours) seem to be fully consistent with the predictions of CDM models of large-scale structure evolution (Daddi et al. 2003 in preparation).

It is also important to stress that the K20 survey allows us to perform tests

which are sensitive to the evolutionary “modes” of galaxies rather than to their formation mechanism. This means that merging, as the main galaxy formation mechanism, is not ruled out by the present observations. Also, it should be noted that PLE models are not a physical alternative to the HMMs, but rather tools useful to parameterize the evolution of galaxies under three main assumptions: high formation redshift, conservation of number density through cosmic times, and passive and luminosity evolution of the stellar populations.

Thus, if we still accept the Λ CDM scenario of hierarchical merging of dark matter halos as the *basic framework* for structure and galaxy formation, the observed discrepancies highlighted by the K20 survey may be ascribed to how the baryon assembly, the star-formation

Figure 10: Left panel: $R - K_s$ colours vs. rest-frame absolute K_s magnitudes for $z = 1.05$ GIF simulated catalogue (small dots) and data (circles) at $0.75 < z < 1.3$ ($z_{\text{mean}} = 1$) (empty and filled circles refer to $z < 1$ and $z > 1$ respectively). Vertical dashed line represents approximately the completeness magnitude limit of GIF catalogue corresponding to its mass limit (see text). Right panel: Colour distribution of luminous galaxies ($M_{K_s} - 5 \log h_{70} < -24.5$) observed (dotted line) and simulated (continuous line), normalized to the same comoving volume.



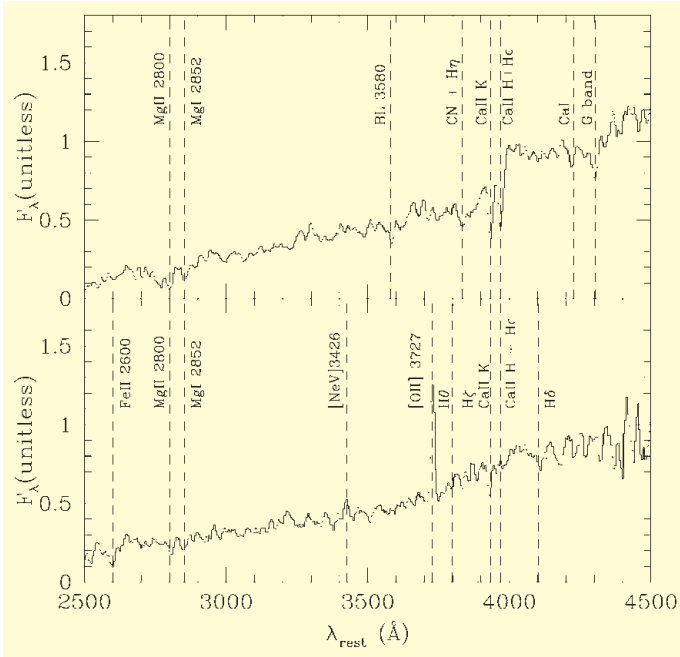


Figure 11: The average rest-frame spectra of old passively evolving (top; $z_{\text{mean}} = 1.000$) and dusty star-forming EROs (bottom; $z_{\text{mean}} = 1.096$) with $K_s \leq 20$ (Cimatti et al. 2002a).

References

- Baugh C.M. et al. 2002, in proceedings 'The Mass of Galaxies at Low and High Redshift', Venice 2001, eds. R. Bender, A. Renzini, astro-ph/0203051.
- Broadhurst, T., Ellis, R.S., & Graebrook, K. 1992, *Nature*, **355**, 55.
- Cimatti A., Daddi E., Mignoli M. et al. 2002a, *A&A*, **381**, L68.
- Cimatti A., Pozzetti L., Mignoli M., et al. 2002b, *A&A*, **391**, L1.
- Cimatti A., Mignoli M., Daddi E. et al. 2002c, *A&A*, **392**, 395.
- Cohen J.G., Blandford R., Hogg D.W. et al. 1999, *ApJ*, **512**, 30.
- Cole S., Lacey C.G., Baugh C.M. & Frenk C.S. 2000, *MNRAS*, **319**, 168.
- Cole S., Norberg P., Baugh C.M. et al. 2001, *MNRAS*, **326**, 255.
- Cowie, L.L., Songaila A., Hu E.M. & Cohen J.G. 1996, *AJ*, **112**, 839.
- Daddi E., Cimatti A., Broadhurst T. et al. 2002, *A&A*, **384**, L1.
- Dickinson M., Papovich C., Ferguson H.C., Budavari T. 2003, *ApJ*, in press, astro-ph/0212242.
- Gavazzi G., Pierini D. & Boselli A. 1996, *A&A*, **312**, 397.
- Giacconi R., Rosati P., Tozzi P. et al. 2001, *ApJ*, **551**, 624.
- Kauffmann G., Charlot S. 1998, *MNRAS*, **297**, L23.
- Kauffmann G. et al. 1999, *MNRAS*, **303**, 188.
- Menci N., Cavaliere A., Fontana A., Giallongo E. & Poli F. 2002, *ApJ*, **575**, 18.
- Peebles P.J.E. 2002, astro-ph/0201015.
- Pozzetti L. Bruzual A.G. & Zamorani, G. 1996, *MNRAS*, **281**, 953.
- Pozzetti L. et al. 2003, *A&A*, in press.
- Renzini A. 1999, in *The Formation of Galactic Bulges*, ed. C.M. Carollo, H.C. Ferguson, & R.F.G. Wyse (Cambridge: CUP), p. 9.
- Somerville R.S., Primack J.R. & Faber S.M. 2001, *MNRAS*, **320**, 504.
- Totani T., Yoshii Y., Maihara T., Iwamuro F. & Motohara K. 2001, *ApJ*, **559**, 592.
- White S.D.M., Rees M.J. 1978, *MNRAS*, **183**, 341.

processes and their feedback are treated by HMMs both within individual galaxies and in their environment. Our results suggest that HMMs should have galaxy formation in a CDM-dominated universe that closely mimics the old-fashioned monolithic collapse scenario. This requires enhanced merging and star formation in massive halos at high redshift (say, $z > 2-3$), and also suppressed star formation in low-mass halos.

In summary, the redshift distribution of $K_s < 20$ galaxies, together with the space density, nature, and clustering properties of the ERO population, and the redshift evolution of the rest-frame near-IR luminosity function and luminosity density provide a new invaluable set of observables on the galaxy population in the $z \sim 1-2$ universe, thus bridging the properties of $z \sim 0$ galaxies with those of Lyman-break and sub-mm/mm-selected galaxies at $z \geq 2-3$. This set of observables poses a new challenge for theoretical models to properly reproduce.

The K20 survey is triggering several studies in which our team is actively involved. Ultradeep spectroscopy was obtained in November 2002 with FORS2 (MXU mode and with the new red-optimized MIT CCD mosaic) in order to derive the redshifts and the nature of the previously unidentified EROs, to increase the spectroscopic redshift completeness of the whole K20 sample, and to study (with higher resolution spectroscopy) the kinematics of $z > 1$ galaxies in order to estimate their dynamical masses. Since the sub-area of the CDFS observed in the K20 survey is also a target of the HST+ACS GOODS Treasury Programme (PI M. Giavalisco), and of the SIRTf GOODS (PI M. Dickinson) and SWIRE (PI C.

Lonsdale) Legacy Programmes, the K20 database, complemented by such additional observations, will allow us to derive new constraints on the formation and evolution of galaxies out to higher redshifts.

We thank the VLT support astronomers for their competent assistance during the observations. AC warmly thanks ESO (Garching) for the hospitality during his visits, and Jim Peebles and Mark Dickinson for useful and stimulating discussions. We also thank Piero Rosati and Mario Nonino for providing the reduced and calibrated *BVRI*/FORs1 images of the CDFS, and C. Baugh, R. Somerville and T. Totani for providing their model predictions.

Figure 12: The average spectra of EROs (black) compared to template spectra (red) of Bruzual & Charlot simple stellar population (top panel), and of dusty starbursts (Kinney et al. 1996, middle panel; Poggianti & Wu 2000, bottom panel).

